ADVANCED MATERIALS
www.advmat.de

Single-Layer Organic Light-Emitting Diode with Trap-Free Host Beats Power Efficiency and Lifetime of Multilayer Devices

*Oskar Sachnik, Yutaka Ie, Naoki Ando, Xiao Tan, Paul W.M. Blom, and Gert-Jan A.H. Wetzelaer**

Organic light-emitting diodes (OLEDs) employing a single active layer potentially offer a number of benefits compared to multilayer devices; reduced number of materials and deposition steps, potential for solution processing, and reduced operating voltage due to the absence of heterojunctions. However, for single-layer OLEDs to achieve efficiencies approaching those of multilayer devices, balanced charge transport is a prerequisite. This requirement excludes many efficient emitters based on thermally activated delayed fluorescence (TADF) that exhibit electron trapping, such as the green-emitting bis(4-(9,9-dimethylacridin-10(9*H*)-yl)phenyl)methanone (DMAC-BP). By employing a recently developed trap-free large band gap material as a host for DMAC-BP, nearly balanced charge transport is achieved. The single-layer OLED reaches an external quantum efficiency (EQE) of 19.6%, which is comparable to the reported EQEs of 18.9–21% for multilayer devices, but achieves a record power efficiency for DMAC-BP OLEDs of 82 lm W^{-1}, clearly surpassing the reported multilayer power efficiencies of 52.9–59 lm W^{-1}. In addition, the operational stability is greatly improved compared to multilayer devices and the use of conventional host materials in combination with DMAC-BP as an emitter. Next to the obvious reduction in production costs, single-layer OLEDs therefore also offer the advantage of reduced energy consumption and enhanced stability.

1. Introduction

In the last decade, organic light-emitting diodes (OLEDs) have become the dominating technology for displays of mobile applications, such as phones and tablets. The achieved high external quantum efficiencies (EQEs) in the 20–30% range are the result of a number of developments, including the harvesting of dark triplet excitons via phosphorescence and efficient charge injection by using doped injection layers.[1–3] Furthermore, to compensate for imbalanced charge transport, charge-blocking layers are employed, which confine electrons and holes in the emissive layer that typically employs a host–guest structure.[4,5] To avoid diffusion of excitons to neighboring layers, exciton-blocking layers with a high triplet energy are employed as well.[6,7] Consequently, a typical multilayer OLED consists of 5–6 layers with a total of 6–8 different organic molecules. In recent research, in order to avoid the use of rare and expensive heavy-metal containing phosphorescent emitters, all-organic emitters exhibiting thermally activated delayed fluorescence (TADF) have been developed as an alternative method to harvest triplet excitons.[8] By a reduction of the overlap between the highest occupied (HOMO) and lowest unoccupied molecular orbitals (LUMO) the energetic splitting between the singlet and triplet energy is strongly reduced, enabling a conversion from triplets to singlets by thermal energy. So far, OLEDs based on these TADF emitters employ the same multilayer device structure as used for phosphorescent emitters.[9–11] As a result, there is a general consensus that such a multilayer structure is a prerequisite for achieving highly efficient OLEDs. Achieving simultaneous efficient charge injection, high electroluminescence quantum yield, absence of exciton quenching at the electrodes and balanced transport in just one active layer is deemed unrealistic.

An OLED with a single-layer architecture, however, could potentially have a number of advantages over multilayer OLEDs. First, the number of organic compounds would be strongly reduced from 6–8 to only 1 or 2. Next to the absence of intermittent evaporation steps and cross contamination prevention, this

O. Sachnik, X. Tan, P. W. Blom, G.-J. A. Wetzelaer
Max Planck Institute for Polymer Research
Ackermannweg 10, 55128 Mainz, Germany
E-mail: wetzelaer@mpip-mainz.mpg.de
Y. Ie, N. Ando
Department of Soft Nanomaterials
Nanoscience and Nanotechnology Center
The Institute of Scientific and Industrial Research
Osaka University
8-1 Mihogaoka, Osaka, Ibaraki 567-0047, Japan

The ORCID identification number(s) for the author(s) of this article can be found under https://doi.org/10.1002/adma.202311892

DOI: 10.1002/adma.202311892

would also allow printing of the active layer without stack integrity issues, which combined will give a cost advantage. Furthermore, the spreading of the emission zone over the complete device structure as compared to the recombination confinement in a thin layer could be beneficial for the device stability due to the reduced local exciton and charge carrier concentrations.[12–16] This would reduce degradation effects originating from exciton–exciton and/or exciton–polaron annihilation.[17–23] The absence of charge blocking layers will also enable charge carriers to travel through the OLED without the obstruction of charge blocking layers, which is beneficial for the operating voltage.[24–26] In case of an equal EQE this would result in a higher power efficiency, which is relevant for portable applications. The big "if", however, is the question whether EQEs comparable to state-of-the-art multilayer OLEDs can be reached by a device employing only one organic active layer. In recent years, the prerequisites to obtain high efficiencies in a single layer OLED have been investigated. Here, fluorescent polymer-based LEDs (PLEDs) have been used as a workhorse. For a PLED based on the conjugated polymer super-yellow poly(phenylene-vinylene) (SY-PPV) it was found that the EQE of 4% is the result of a combination of direct electron-hole recombination (2.5%) and triplet–triplet annihilation (TTA) (1.5%). Since TTA is a loss process in TADF-based OLEDs the addition of a triplet harvesting functionality would only increase the EQE to a maximum of 10%.[27] Further enhancement of the efficiency requires the elimination of electron trapping, which has a triple negative effect on the EQE. First, the non-radiative recombination of trapped electrons with free holes is a loss process, lowering the electrical efficiency in the range of 70–80%.[28] Furthermore, also the photoluminescence quantum yield is lowered to 65% since singlet excitons dissociate at the electron traps.[29] Finally, the resulting confinement of the recombination zone close to the cathode lowers the optical outcoupling efficiency.[30] Elimination of the electron trapping would enhance the maximum attainable efficiency then from 10% to the 27–28% range for a single-layer device, which would be on par with the multilayer OLEDs. An essential step is therefore the elimination of trapping effects.

In a recent study, it was demonstrated that for organic semiconductors a trap-free energy window exists with a width of 2.5 eV.[31] Semiconductors with an electron affinity lower than 3.5 eV are susceptible to electron trapping, whereas an ionization energy larger than 6 eV gives rise to hole trapping. For trap-free bipolar charge transport, both energy levels have to be inside this energy window. This, however, puts a fundamental challenge on the realization of trap-free organic semiconductors with a band gap larger than 2.5 eV, as required for blue OLEDs. Another important condition for realizing efficient single-layer OLEDs is the realization of Ohmic contacts. Not only is efficient charge injection beneficial for the efficiency and operating voltage of the OLED, but the resulting band bending due to the accumulated charges near the Ohmic contact prevents the minority carrier to leave the device without recombining.[32] In this way, Ohmic contacts additionally prevent recombination close to the metallic electrode, avoiding outcoupling losses due to energy transfer to surface-plasmon-polariton modes.[33,34] It was found that Ohmic contacts on nearly any organic semiconductor can be realized by the combination of a tunnel barrier with a metal-oxide electrode.[35] Here, the tunnel barrier electrostatically decouples the electrode from the semiconductor. Using this injection strategy combined with the energetic demands for trap-free bipolar transport, an OLED based on the yellow TADF emitter 5,10-bis(4-(9*H*-carbazol-9-yl)phenyl)-5,10-dihydroboranthrene (CzDBA) was fabricated.[36] The OLED comprised a simplified structure consisting of two tunnel barriers and an active layer of CzDBA, which has the relevant energy levels exactly at the edges of the trap-free window. Due to the resulting nearly trap-free electron and hole transport combined with Ohmic contacts, an EQE of 19% was achieved.

The fact that the realization of bipolar trap-free transport puts stringent demands on the energy levels of TADF emitters excludes many well-known materials for the realization of efficient single-layer OLEDs. One such example is the green emitter bis(4-(9,9-dimethylacridin-10(9*H*)-yl)phenyl)methanone (DMAC-BP).[37] Employed in doped and non-doped multilayer OLED stacks, EQEs in the range 19–21% have been reported, together with (maximum) power efficiencies of 52.9-59 lm W^{-1}.[37–39]

Here, we demonstrate a new concept of using a trap-free host material in a single-layer DMAC-BP-based OLED. Due to the unrivalled electron transport of the trap-free host, balanced charge transport and high mobilities are achieved for both electrons and holes. Direct charge injection into the emissive layer with the single-layer architecture, together with efficient bipolar charge transport results in very low operating voltages, giving rise to record-high power efficiencies for DMAC-BP OLEDs, clearly surpassing the best multilayer OLEDs based on this emitter. The spreading of the emission zone due to both the single-layer architecture and the trap-free host further results in greatly enhanced operational stability.

2. Results and Discussion

As good and balanced charge transport is a prerequisite for single-layer OLEDs, we first investigate the charge transport in pristine DMAC-BP. In **Figure 1a**, the electron and hole current density versus voltage (*J*–*V*) in a pristine DMAC-BP film is shown, obtained using electron- and hole only devices. Details of the devices and their processing are given in the Experimental Section.

The charge transport is highly imbalanced, which is expected given the position of the HOMO and LUMO levels of −5.6 and −2.7 eV, respectively. Here, the HOMO level is within the trap-free window, whereas the LUMO level is far outside, resulting in severe electron trapping. For the OLED of pristine DMAC-BP, we make use of a spin-coated PEDOT:PSS anode, of which the work function is enhanced by blending it with perfluorinated ionomers (PFI).[40] Such a solution-processed PEDOT:PSS:PFI anode was recently shown to form Ohmic contacts on CzDBA with an IE as high as 5.9 eV, without the need for a tunnel barrier.[41] For the electron injection a Ba/Al electrode was used in combination with a thin TPBi (4 nm) tunnel barrier. Although a thick TPBi layer has the potential to function as a hole-blocking and exciton-blocking layer, a 4 nm layer is not sufficient to prevent energy transfer of excitons to the metallic top electrode.[42] Furthermore, it has been demonstrated that tunneling layers in this thickness range are transparent for holes.[35] Therefore, the TPBi interlayer only facilitates electron injection, while not exhibiting a

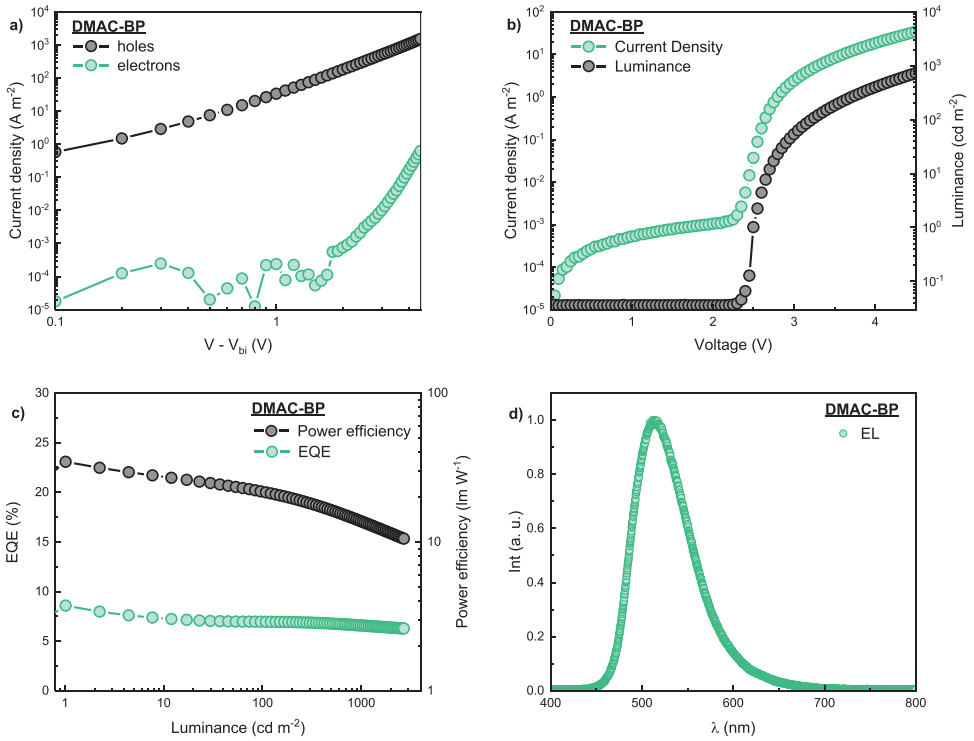

Figure 1. a) Current–density versus voltage (*J*–*V*) characteristics for electrons (green symbols) and holes (black symbols) for a pristine DMAC-BP film of 100 nm thickness. The electron-only device was corrected for a built-in voltage of V_{bi} = 0.68 V. b) Current density (green symbols) and luminance (black symbols) versus voltage for a single-layer DMAC-BP OLED with 144 nm thickness. c) External quantum efficiency (EQE) (green symbols) and power efficiency (black symbols) for a single layer DMAC-BP OLED.

blocking function like in multilayer OLEDs. As such, the OLED can be classified as a single-layer OLED, in which the use of thin injection layers is common practice. In Figure 1b,c, the *J*–*V* and luminance–voltage (*L*–*V*) characteristics are shown for a pristine DMAC-BP OLED. As expected, due to the strong electron trapping and resulting confinement of the emission zone close to the cathode the maximum EQE and power efficiency of the OLED amount to only 8% and 32 lm W^{-1}, respectively.

In a recent study, a bottom-up strategy was presented to avoid trapping in organic semiconductors with a band gap larger than 2.5 eV. By spatially separating the HOMO and LUMO orbitals and tuning the stacking of the molecules by chemical modification, the LUMO orbitals can be spatially protected from electron-trapping impurities. For the compound 9,9′,9″-(5-(4,6-diphenyl-1,3,5-triazin-2-yl)benzene-1,2,3-triyl)tris(9*H*-carbazole) (3CzTRZ), the electron current was observed to be nearly trap free, in spite of the LUMO being outside of the trap-free window.[43] Such a large band gap trap-free organic semiconductor is ideally suited to be used as a host for TADF emitters with imbalanced transport, such as DMAC-BP. In **Figure 2**a the energy levels of DMAC-BP and 3CzTRZ are schematically indicated. 3CzTRZ has a HOMO level of −5.8 eV and a LUMO level of −2.9 eV.[43] In a DMAC-BP:3CzTRZ blend in near equal ratios, the electron transport will take place in the 3CzTRZ, whereas the hole transport is governed by the DMAC-BP, resulting in nearly trap-free transport for both carriers. The offset between the LUMO levels was verified by using inverse photoelectron spectroscopy (IPES) (Figure S4, Supporting Information).[44] In Figure 2b, the electron and hole current for a 40:60 DMAC-BP:3CzTRZ blend are shown.

For this blend ratio, the electron and hole transport is perfectly balanced and nearly trap free, as evidenced by the quadratic dependence of the current on voltage, characteristic of a trap-free space-charge-limited current. The applied voltage for the electron-only device was corrected for a built-in voltage of V_{bi} = 0.69 eV. When the amount of DMAC-BP is further reduced to 10% the electron current in the 3CzTRZ becomes dominant over the hole current in the strongly diluted DMAC-BP, again resulting in imbalanced transport (now electron dominated), see Figure S1a (Supporting Information).

As a next step, we have fabricated OLEDs based on the 40:60 DMAC-BP:3CzTRZ blend with a PEDOT:PSS:PFI anode and TPBi(4 nm)/Ba/Al cathode. In **Figure 3**a the *J*–*V* and *L*–*V* characteristics are shown, together with the EQE and power efficiency (Figure 3b).

As shown in Figure 3b, the maximum EQE of the 40:60 DMAC-BP:3CzTRZ blend OLED is strongly enhanced up to 19.6% for the optimal layer thickness (see Figures S6 and S7, Supporting Information). This EQE is similar to the reported values in the range of 19–21% for multilayer OLEDs with DMAC-BP as the emitter.[37–39] However, the reduced operating voltage of the single-layer device due to the absence of charge-blocking layers, reaching 1,000 cd m^{-2} already at 2.95 V, results in a superior maximum power efficiency of 82 and 77.8 lm W^{-1} at a luminance of 100 cd m^{-2}. The single-layer OLED strongly outperforms the power efficiencies of multilayer OLEDs,[37–39] with

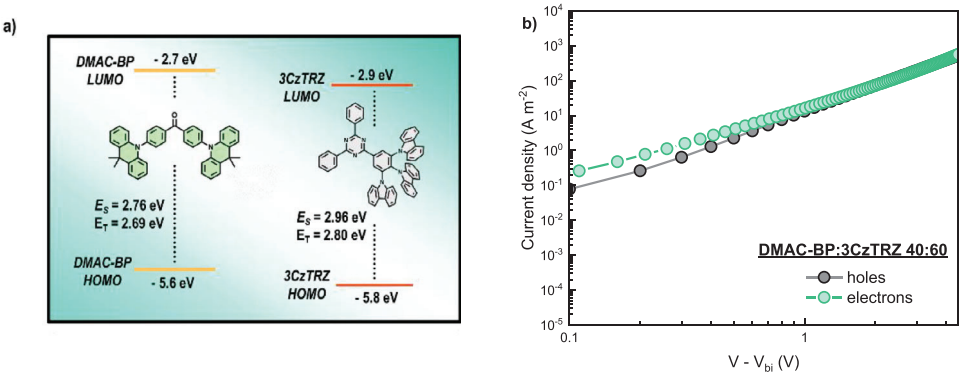

Figure 2. a) Energy band diagram of DMAC-BP and 3CzTRZ and indicated singlet and triplet levels.[37,45] b) Current–density versus voltage (*J*–*V*) characteristics for electrons (green symbols) and holes (black symbols) for a film consisting of a 40:60 DMAC-BP:3CzTRZ blend of 70 nm thickness. The electron-only was corrected for a built-in voltage of V_{bi} = 0.69 V.

the maximum reported value being 59 lm W^{-1} at 100 cd m^{-2}.[37] Even at a high luminance of 5,000 cd m^{-2}, the power efficiency is still 41.7 lm W^{-1}, which is higher than the best reported value of 25.7 lm W^{-1} at the same luminance, the latter being achieved for a multilayer device using DMIC-TRZ as a host for DMAC-BP in the emissive layer.[39] In **Figure 4a** schematics of the device structure and (power) efficiencies of the various OLEDs are shown for comparison. This result demonstrates that single-layer OLEDs are capable of outperforming multilayer devices employing the same TADF emitter.

The use of a trap-free host to achieve balanced charge transport not only positively affects the efficiency, but also the lifetime. As shown in Figure 3d, the LT_{50} lifetime of the 40:60 DMAC-BP:3CzTRZ blend OLED reaches 41 h at an initial luminance of 1,000 cd m^{-2}, while the single-layer OLED based on neat DMAC-BP achieves a lifetime of 10 h. In a multilayer OLED, a lifetime of under 4 h has been reported for non-doped DMAC-BP, while the lifetime is limited to only 30 min when using a conventional host.[37] As a result, it is demonstrated that both the use of 3CzTRZ as a host, as well as the use of the single-layer device

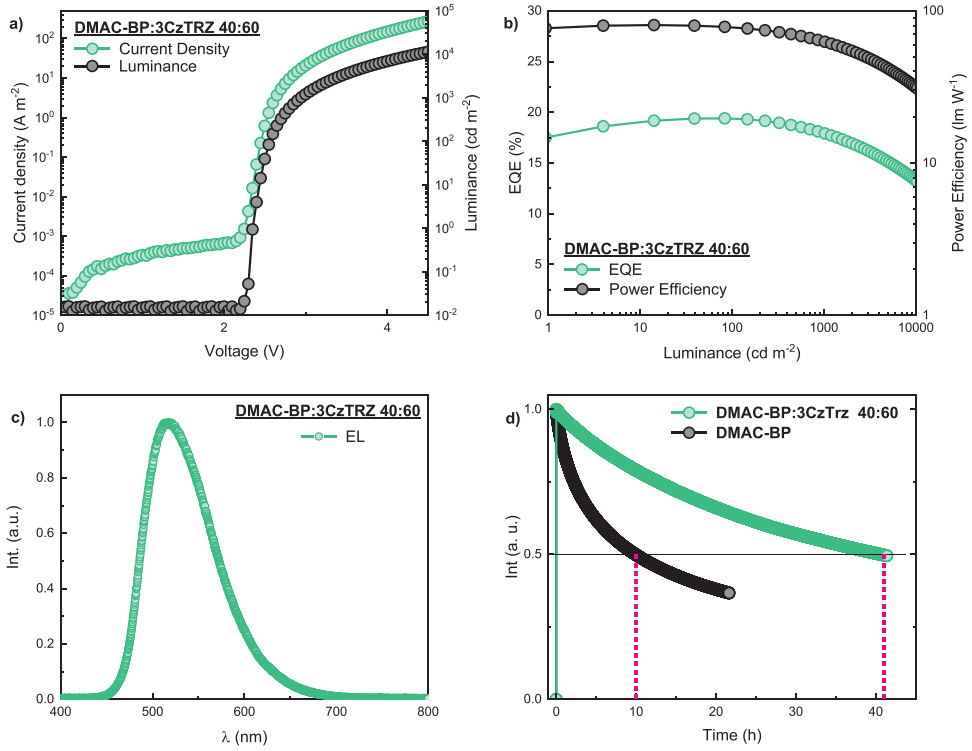

Figure 3. a) Current density (green symbols) and luminance (black symbols) versus voltage for a 40:60 DMAC-BP:3CzTRZ blend OLED with 70 nm thickness. b) External quantum efficiency (EQE) (green symbols) and power efficiency (black symbols) for the 40:60 DMAC-BP:3CzTRZ blend OLED. c) The observed electroluminescence spectrum for the DMAC-BP:3CzTRZ 40:60 based OLED. d) Lifetime measurements of pure DMAC-BP and DMAC-BP:3CzTRZ (40:60) at 1,000 cd m^{-2} initial luminance.

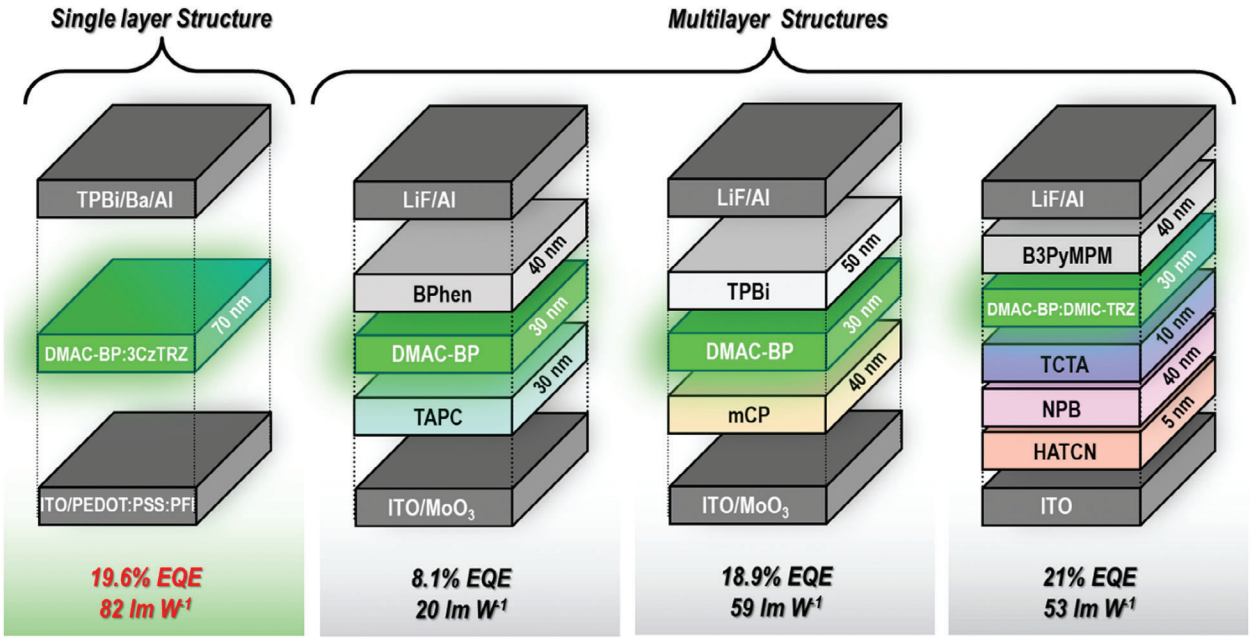

Figure 4. Schematic diagram of the single-layer OLED used in this study and multilayer OLEDs reported in literature with the corresponding maximum EQE and maximum power efficiency.

concept vastly improves the device stability. The use of a single-layer device architecture with a thick emissive layer allows for broadening of the emission zone, which is optimally achieved for balanced charge transport, as is obtained here with the use of the trap-free host material. The broadened emission zone reduces the interaction between excitons and polarons, finally resulting in greatly improved operational stability.

Upon reducing the emitter concentration in the DMAC-BP:3CzTRZ blend, the charge transport becomes electron dominated. This is expected, since hole-transport takes place on DMAC-BP, and a lower concentration reduces guest-to-guest hopping. For OLEDs consisting of a 10:90 DMAC-BP:3CzTRZ blend the performance decreases due to the loss of the balanced transport (Figure S1, Supporting Information). However, with a maximum EQE of 14% these OLEDs still outperform the pristine DMAC-BP OLEDs. The reason is that in the electron-dominated 10:90 DMAC-BP:3CzTRZ OLED the recombination zone is far away from the metallic cathode and close to the PEDOT:PSS:PFI anode, resulting in lower losses due to coupling of photons to surface-plasmon modes. On the other hand, in a 50:50 ratio, the OLED becomes slightly hole dominated (Figure S2, Supporting Information). The slight loss of charge balance reduces the EQE compared to the optimum 40:60 DMAC-BP:3CzTRZ ratio.

To further investigate the relevance of the use of a trap-free large band gap host like 3CzTRZ, as a reference a single-layer OLED using the well-known wide-gap host 9-(3-(9*H*-carbazol-9-yl)phenyl)-9*H*-carbazole-3-carbonitrile (mCPCN) is investigated, using a blend ratio of 1:1 with DMAC-BP.[41,46,47] For the host mCPCN with the HOMO at −5.80 eV and LUMO at −2.24 eV the electron and hole transport will both take place on DMAC-BP, resulting again in imbalanced transport. As shown in **Figure 5a** the electron and hole transport is indeed strongly imbalanced, although the balance is improved as compared to pristine DMAC-BP. This might be the result of the trap-dilution effect that

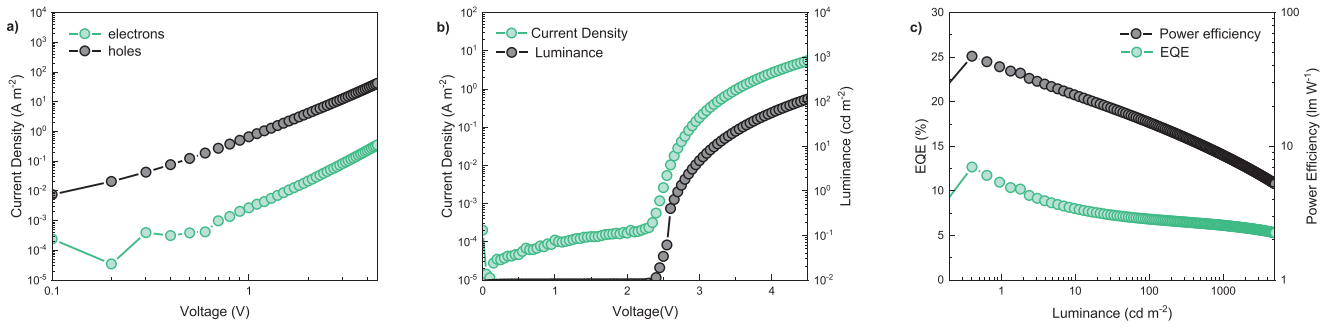

Figure 5. a) Current–density versus voltage (*J*–*V*) characteristics for electrons (green symbols) and holes (black symbols) for a film consisting of a DMAC-BP:mCPCN 1:1 blend of 94 nm thickness. The applied voltage for the electron-only device was corrected for a built-in voltage of V_{bi} = 0.70 V. b) External quantum efficiency (EQE) (green symbols) and power efficiency (black symbols) for a single layer DMAC-BP:mCPCN 1:1 OLED.

modifies the statistics between free and trapped carriers.[48] The resulting EQE and power efficiency of the DMAC-BP:mCPCN (Figure 5b) are therefore in between those of the pristine DMAC-BP and 40:60 DMAC-BP:3CzTRZ devices, amounting to a maximum of 13% and 50 lm W^{-1}, respectively. However, the reduced charge transport has a strong negative impact on the operating voltage. As a result, the power efficiency only amounts to 15.0 lm W^{-1} at a luminance of 100 cd m^{-2}. This result confirms the relevance of applying a trap-free host to obtain balanced transport and high power efficiency in TADF OLEDs.

We also investigated the use of 2CzTRZ as a host, which has a similar LUMO energy as 3CzTRZ, but shows some electron trapping.[43] As a result, electron transport takes place via 2CzTRZ, so that the impact of electron trapping in the host material can be investigated. As shown in Figure S8 (Supporting Information), the electron transport is clearly lower than the hole transport at low voltage, which is due to electron trapping. Since the electron-trap density in 2CzTRZ is still in the lower range for organic semiconductors, a transition to the trap-filled limit occurs at a voltage within the OLED operation window. Therefore, at higher voltages the charge transport becomes balanced. This is also reflected in the EQE (Figure S9, Supporting Information) of the single-layer OLED of the DMAC-BP:2CzTRZ blend, which is low at low luminance due charge imbalance, while it increases to decent levels at higher luminance due to more balanced transport. We note that for hosts with more severe trapping, as is common in organic semiconductors, the EQE will be heavily compromised.

3. Conclusion

In conclusion, we have demonstrated that a trap-free wide band gap organic semiconductor such as 3CzTRZ can be used to achieve balanced charge transport in intrinsically trap-limited emitters such as DMAC-BP. Balanced charge transport is a prerequisite for the use of organic emitters in a single-layer OLED to attain a decent device performance. We demonstrate that single-layer OLEDs employing a trap-free host can surpass the performance of current multilayer OLED architectures, by virtue of a lower operating voltage due to improved charge transport and the absence of heterojunctions within the stack. Exhibiting a similar EQE to multilayer devices, the lower operating voltage results in drastically improved power efficiencies. The obtained power efficiency (max 82 lm W^{-1}) represents a record for DMAC-BP OLEDs, being almost 40% higher than the next most efficient reported device. In addition, we have demonstrated that also the operational stability is greatly improved, due to a better spreading of the emission zone, as a result of both the single-layer architecture and the trap-free host to balance the transport. These results cannot be achieved with conventional host materials, which characteristically exhibit trap-limited charge transport of at least one type of charge carrier, with electron trapping being the most common case.

4. Experimental Section

3CzTRZ was synthesized according to literature and purified by sublimation.[43] Nafion (PFI) was purchased from Sigma Aldrich as 5 wt% solution in a mixture of lower aliphatic alcohols and water, containing 45% water. DMAC-BP, mCPCN, TPBi, and C_{60} were purchased in sublimed grade from Ossila BV.

Device Fabrication: OLED devices were fabricated on glass substrates prepatterned with ITO. The substrates were cleaned by washing with detergent solution and ultrasonication in acetone (5 min) and isopropyl alcohol (5 min), followed by UV–ozone treatment (50 min). PFI-containing blends were prepared 24 h prior to device fabrication by mixing PEDOT:PSS (CLEVIOS P VP AI 4083) with Nafion in a 1:6:14 ratio and diluted in deionized water (1:1). PEDOT:PSS:PFI was applied by spin coating, resulting in films of 20 nm thickness, which were subsequently annealed at 130 °C for 12 min. The substrates were then transferred to a nitrogen-filled glove box. Thermal evaporation of the emissive layer was performed at a base pressure of 2×10^{-6} to 3×10^{-6} mbar. Barium (3 nm) and aluminum (100 nm) were evaporated to finalize the top contact. For hole-only devices, a top contact consisting of C_{60} (4 nm), MoO_3 (7 nm) and aluminum (100 nm) was evaporated. For electron-only devices, aluminum (30 nm) was thermally evaporated on cleaned glass substrates, followed by thermal evaporation of the emissive layer and a TPBi (4 nm) interlayer and the barium (5 nm) and aluminum (100 nm) top contact.

Measurements: Electrical characterization was carried out under nitrogen atmosphere with a Keithley 2400 source meter and light output was recorded with a Si photodiode with NIST-traceable calibration, with a detector area (1 cm^2) larger than the emitting area of the OLED (0.16 cm^2). The photodiode was placed close to (but not in contact with) the OLED to capture all photons emitted in a forward hemisphere. To avoid any light detection emitted from the substrate edges, the edges were masked by the sample holder and the substrate size (3×3 cm^2) was considerably larger than the photodetector area. The EQE, the luminance and power efficiency were calculated from the measured photocurrent, the device current, and the electroluminescence spectrum. Electroluminescence spectra were obtained with a USB4000-UV–VIS-ES spectrometer.

Supporting Information

Supporting Information is available from the Wiley Online Library or from the author.

Acknowledgements

Open access funding enabled and organized by Projekt DEAL.

Conflict of Interest

The authors declare no conflict of interest.

Data Availability Statement

The data that support the findings of this study are available from the corresponding author upon reasonable request.

Keywords

charge transport, device physics, organic light-emitting diodes, thermally activated delayed fluorescence

Received: November 9, 2023
Published online: January 12, 2024

[1] M. A. Baldo, D. F. O'brien, Y. You, A. Shoustikov, S. Sibley, M. E. Thompson, S. R. Forrest, *Nature* **1998**, *395*, 151.

[2] K. Walzer, B. Maennig, M. Pfeiffer, K. Leo, *Chem. Rev.* **2007**, *107*, 1233.
[3] M. Furno, R. Meerheim, S. Hofmann, B. Lüssem, K. Leo, *Phys. Rev. B: Condens. Matter Mater. Phys.* **2012**, *85*, 115205.
[4] H. Sasabe, N. Toyota, H. Nakanishi, T. Ishizaka, Y.-J. Pu, J. Kido, *Adv. Mater.* **2012**, *24*, 3212.
[5] J. Kido, M. Kimura, K. Nagai, *Science* **1995**, *267*, 1332.
[6] J.-A. Seo, S. K. Jeon, M. S. Gong, J. Y. Lee, C. H. Noh, S. H. Kim, *J. Mater. Chem. C* **2015**, *3*, 4640.
[7] C.-H. Shih, P. Rajamalli, C.-A. Wu, W.-T. Hsieh, C.-H. Cheng, *ACS Appl. Mater. Interfaces* **2015**, *7*, 10466.
[8] H. Uoyama, K. Goushi, K. Shizu, H. Nomura, C. Adachi, *Nature* **2012**, *492*, 234.
[9] S. O. Jeon, K. H. Lee, J. S. Kim, S.-G. Ihn, Y. S. Chung, J. W. Kim, H. Lee, S. Kim, H. Choi, J. Y. Lee, *Nat. Photonics* **2021**, *15*, 208.
[10] L.-S. Cui, A. J. Gillett, S.-F. Zhang, H. Ye, Y. Liu, X.-K. Chen, Z.-S. Lin, E. W. Evans, W. K. Myers, T. K. Ronson, H. Nakanotani, S. Reineke, J.-L. Bredas, C. Adachi, R. H. Friend, *Nat. Photonics* **2020**, *14*, 636.
[11] J. Sun, H. Ahn, S. Kang, S.-B. Ko, D. Song, H. A. Um, S. Kim, Y. Lee, P. Jeon, S.-H. Hwang, Y. You, C. Chu, S. Kim, *Nat. Photonics* **2022**, *16*, 212.
[12] L. Duan, D. Zhang, K. Wu, X. Huang, L. Wang, Y. Qiu, *Adv. Funct. Mater.* **2011**, *21*, 3540.
[13] S. J. Lee, J. R. Koo, H. W. Lee, S. E. Lee, H. J. Yang, S. S. Yoon, J. Park, Y. K. Kim, *Electron. Mater. Lett.* **2014**, *10*, 1127.
[14] S. J. Lee, S. E. Lee, D. H. Lee, J. R. Koo, H. W. Lee, S. S. Yoon, J. Park, Y. K. Kim, *Jpn. J. Appl. Phys.* **2014**, *53*, 101601.
[15] T.-H. Han, Y.-H. Kim, M. H. Kim, W. Song, T.-W. Lee, *ACS Appl. Mater. Interfaces* **2016**, *8*, 6152.
[16] J. S. Bangsund, K. W. Hershey, D. C. K. Rathwell, H.-Y. Na, J.-H. Jeon, P. Trefonas, R. J. Holmes, *J. Soc. Inf. Disp.* **2019**, *27*, 434.
[17] B. Van Der Zee, Y. Li, G.-J. A. H. Wetzelaer, P. W. M. Blom, *Phys. Rev. Appl.* **2022**, *18*, 064002.
[18] R. Coehoorn, H. Van Eersel, P. Bobbert, R. Janssen, *Adv. Funct. Mater.* **2015**, *25*, 2024.
[19] C. Zhao, L. Duan, *J. Mater. Chem. C* **2020**, *8*, 803.
[20] R. Mac Ciarnáin, H. W. Mo, K. Nagayoshi, H. Fujimoto, K. Harada, R. Gehlhaar, T. H. Ke, P. Heremans, C. Adachi, *Adv. Mater.* **2022**, *34*, 2201409.
[21] T.-Y. Cheng, J.-H. Lee, C.-H. Chen, P.-H. Chen, P.-S. Wang, C.-E. Lin, B.-Y. Lin, Y.-H. Lan, Y.-H. Hsieh, J.-J. Huang, H.-F. Lu, I. Chao, M.-K. Leung, T.-L. Chiu, C.-F. Lin, *Sci. Rep.* **2019**, *9*, 3654.
[22] J. Wu, L. Ameri, L. Cao, J. Li, *Appl. Phys. Lett.* **2021**, *118*, 073301.
[23] T. Xu, M. Yang, J. Liu, X. Wu, I. Murtaza, G. He, H. Meng, *Org. Electron.* **2016**, *37*, 93.
[24] M. E. Kondakova, T. D. Pawlik, R. H. Young, D. J. Giesen, D. Y. Kondakov, C. T. Brown, J. C. Deaton, J. R. Lenhard, K. P. Klubek, *J. Appl. Phys.* **2008**, *104*, 094501.
[25] S. J. Cha, Y. R. Cho, M. C. Suh, *Synth. Met.* **2015**, *200*, 143.
[26] J. Lee, J.-I. Lee, J. Y. Lee, H. Y. Chu, *Appl. Phys. Lett.* **2009**, *94*, 193305.
[27] B. Van Der Zee, Y. Li, G.-J. A. H. Wetzelaer, P. W. M. Blom, *Adv. Mater.* **2022**, *34*, 2108887.
[28] M. Kuik, L. J. A. Koster, A. G. Dijkstra, G. A. H. Wetzelaer, P. W. M. Blom, *Org. Electron.* **2012**, *13*, 969.
[29] I. Rörich, A.-K. Schönbein, D. K. Mangalore, A. Halda Ribeiro, C. Kasparek, C. Bauer, N. I. Craciun, P. W. M. Blom, C. Ramanan, *J. Mater. Chem. C* **2018**, *6*, 10569.
[30] Y. Li, N. B. Kotadiya, B. Van Der Zee, P. W. M. Blom, G.-J. A. H. Wetzelaer, *Adv. Opt. Mater.* **2021**, *9*, 2001812.
[31] N. B. Kotadiya, A. Mondal, P. W. M. Blom, D. Andrienko, G.-J. A. H. Wetzelaer, *Nat. Mater.* **2019**, *18*, 1182.
[32] G.-J. A. H. Wetzelaer, P. W. M. Blom, *ACS Appl. Mater. Interfaces* **2022**, *14*, 7523.
[33] R. Meerheim, M. Furno, S. Hofmann, B. Lüssem, K. Leo, *Appl. Phys. Lett.* **2010**, *97*, 253305.
[34] C. Fuchs, P.-A. Will, M. Wieczorek, M. C. Gather, S. Hofmann, S. Reineke, K. Leo, R. Scholz, *Phys. Rev. B: Condens. Matter Mater. Phys.* **2015**, *92*, 245306.
[35] N. B. Kotadiya, H. Lu, A. Mondal, Y. Ie, D. Andrienko, P. W. M. Blom, G.-J. A. H. Wetzelaer, *Nat. Mater.* **2018**, *17*, 329.
[36] N. B. Kotadiya, P. W. M. Blom, G.-J. A. H. Wetzelaer, *Nat. Photonics* **2019**, *13*, 765.
[37] Q. Zhang, D. Tsang, H. Kuwabara, Y. Hatae, B. Li, T. Takahashi, S. Y. Lee, T. Yasuda, C. Adachi, *Adv. Mater.* **2015**, *27*, 2096.
[38] X. Jiang, H. Lin, C. Xue, G. Zhang, W. Jiang, G. Xing, *J. Mater. Sci.* **2020**, *31*, 19136.
[39] D. Zhang, C. Zhao, Y. Zhang, X. Song, P. Wei, M. Cai, L. Duan, *ACS Appl. Mater. Interfaces* **2017**, *9*, 4769.
[40] T.-W. Lee, Y. Chung, O. Kwon, J.-J. Park, *Adv. Funct. Mater.* **2007**, *17*, 390.
[41] O. Sachnik, Y. Li, X. Tan, J. J. Michels, P. W. M. Blom, G.-J. A. H. Wetzelaer, *Adv. Mater.* **2023**, *35*, 2300574.
[42] G. Cnossen, K. E. Drabe, D. A. Wiersma, *J. Chem. Phys.* **1993**, *98*, 5276.
[43] O. Sachnik, X. Tan, D. Dou, C. Haese, N. Kinaret, K.-H. Lin, D. Andrienko, M. Baumgarten, R. Graf, G.-J. A. H. Wetzelaer, J. J. Michels, P. W. M. Blom, *Nat. Mater.* **2023**, *22*, 1114.
[44] N. V. Smith, *Rep. Prog. Phys.* **1988**, *51*, 1227.
[45] D. R. Lee, M. Kim, S. K. Jeon, S.-H. Hwang, C. W. Lee, J. Y. Lee, *Adv. Mater.* **2015**, *27*, 5861.
[46] M.-S. Lin, S.-J. Yang, H.-W. Chang, Y.-H. Huang, Y.-T. Tsai, C.-C. Wu, S.-H. Chou, E. Mondal, K.-T. Wong, *J. Mater. Chem.* **2012**, *22*, 16114.
[47] W. Zeng, H.-Y. Lai, W.-K. Lee, M. Jiao, Y.-J. Shiu, C. Zhong, S. Gong, T. Zhou, G. Xie, M. Sarma, K.-T. Wong, C.-C. Wu, C. Yang, *Adv. Mater.* **2018**, *30*, 1704961.
[48] D. Abbaszadeh, A. Kunz, G. A. H. Wetzelaer, J. J. Michels, N. I. Craciun, K. Koynov, I. Lieberwirth, P. W. M. Blom, *Nat. Mater.* **2016**, *15*, 628.